2015

Characterizing a Shallow Groundwater System beneath Irrigated Sugarcane with Electrical Resistivity and Radon (222Rn), Puunene, Hawai

John Dunbar
Baylor University, john_dunbar@baylor.edu

Peter Allen
Baylor University

Joseph White
Baylor University

Ram Neupane
Baylor University

Tian Xu
Baylor University

See next page for additional authors

Characterizing a Shallow Groundwater System beneath Irrigated Sugarcane with Electrical Resistivity and Radon (^{222}Rn), Puunene, Hawaii

John Dunbar[1], Peter Allen[1], Joseph White[2], Ram Neupane[2], Tian Xu[1], June Wolfe[3] and Jeff Arnold[4]
[1]Baylor University, Department of Geology, One Bear Place #97354, Waco, TX 76798
Email: john_dunbar@baylor.edu
[2]Baylor University, Department of Biology, One Bear Place #97388, Waco, TX 76798
[3]Texas A&M University, AgriLife Research & Extension Center, 720 East Blackland Road, Temple, TX 76502
[4]USDA-ARS, 720 East Blackland Road, Temple, TX 76502

ABSTRACT

In this study, we use a combination of electrical resistivity profiling and radon (^{222}Rn) measurements to characterize a shallow groundwater system beneath the last remaining, large-scale sugarcane plantation on Maui, Hawaii. Hawaiian Commercial & Sugar Company has continuously operated a sugarcane plantation on the western flank of Haleakala Volcano since 1878. The sugarcane is irrigated with a combination of surface water brought through tunnels from the wetter, eastern flank of Haleakala Volcano and groundwater from wells within the plantation. To assess the flow of irrigation water through the shallow subsurface, we collected a representative topo-sequence of four 2-D resistivity profiles that sample different topographic and hydrologic settings within the plantation. The profiles show a down-slope-thickening (0 to 20 m), surficial low-resistivity (10-200 Ohm-m) layer extending from the upslope limit of irrigated sugarcane to the lowest elevations of the plantation. At a canal crossing, the low resistivity layer thickens and is less resistive upslope of the canal. Beneath a reservoir at mid-elevation, the layer thickens to 20 m and curves down slope beneath the reservoir and up to the base of the field beyond. At the base of the slope, the low resistivity layer is 20-m thick below both fields and a second reservoir. An increase in radon concentration in the down-flow direction within the canal system at one location suggests groundwater infiltration into the canal. We attribute the low-resistivity layer to irrigation water that has infiltrated below the root zone and leaked from canals and reservoirs within the plantation. The water flows down slope to the base of the slope and there flows vertically, recharging the basal aquifer. We suggest that seepage from the canals and reservoirs is in part controlled by the local pressure head within the shallow flow system.

Introduction

Irrigation for agricultural purposes accounts for approximately 70% of freshwater use globally (Hotchkiss *et al*., 2001; Wada *et al*., 2013). Demands on freshwater resources have grown over recent decades, resulting in increased competition between municipal, industrial, agricultural and environmental uses for these resources (Khan *et al*., 2006; de Fraiture *et al*., 2010). With increased competition has come economic and political pressure to improve the efficiency of water use within large agricultural systems (Khan *et al*., 2010; Mushtaq *et al*., 2012). To this end, experimentation with near-surface geophysical methods applied to irrigation problems began in the 1950's and 1960's (*e.g.*, Wantland, 1953; McDonald and Wantland, 1960; USDIBR, 1963). Electrical geophysical methods have been the most effective. Various electromagnetic (EM), ground penetrating radar (GPR) and direct current (DC) resistivity systems have been walked, towed and flown along irrigation canals to identify zones of leakage (Engelbert *et al*., 1997; Hotchkiss *et al*., 2001). In more recent studies, geophysical methods have been used to answer the larger questions of how well the irrigation systems work and how irrigation systems interact with and modify the underlying groundwater systems (*e.g.*, Humphreys *et al*., 2002; Watt, 2008; Minsley *et al*., 2010; Dor *et al*., 2011). This study addresses the latter—the interaction of irrigation and subsurface groundwater systems.

Between 2010 and 2013 we investigated a shallow groundwater flow system within the last remaining

 DOI: 10.2113/JEEG20.2.165

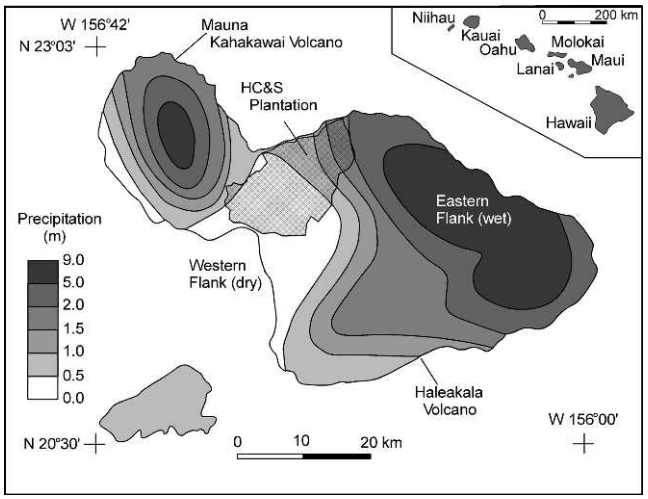

Figure 1. Hawaiian Commercial & Sugar Company plantation location on the western flank of Haleakala Volcano, Maui Island, Hawaii. The plantation is located within the area marked with the hash pattern. The northeast flank of the island, facing the Trade Winds, receives 5 to 9 m of precipitation per year. The southwestern flank is semiarid.

commercial sugarcane plantation on Maui, Hawaii (Fig. 1). Hawaiian Commercial & Sugar Company (HC&S), Pu'unene, Maui, Hawaii maintains 14,380 hectares of sugarcane under drip irrigation. The irrigation system supplies water to the sugarcane fields from a complex network of tunnels and canals that bring surface water from the wetter, eastern flank of Haleakala Volcano to the plantation on the drier western flank. The surface water is augmented on an as needed basis by water pumped from hand-dug wells into the basal aquifer, within the plantation. The basal aquifer contains a freshwater lens floating on saltwater, near sea level. Much of the irrigation water conveyance system dates from the late 1870s and has been maintained without major modifications since that time. Our study was part of a larger project to assess the sustainability of converting a portion of the HC&S sugarcane to alternate crops for biofuels production.

The limiting factor in the sustainability of biofuels production within the HC&S plantation is the continued availability of water into the future. However, the growing population of Maui and interest in maintaining stream flow for wildlife habitat have raised possible alternate uses for the surface water used by HC&S. Furthermore, estimates of future precipitation within mountainous Hawaiian watersheds suggest decreases in stream flow between 7 and 17% may occur over the next 40 yrs because of climate change (Safeeq and Fares, 2012). Either or both of these factors could reduce the availability of surface water to the HC&S plantation in the coming decades. Hence, a major question for the long term management of the HC&S plantation is whether such a decrease could be compensated for by increasing efficiency of the irrigation system, increasing withdraws from the basal aquifer, or some combination of both. Past experience indicates that freshwater levels within the basal aquifer are strongly influenced by plantation management practices. In this regard, an effort is underway to better constrain how much water is lost from different parts of the irrigation water conveyance system. This is done by measuring the loss rates from representative samples of the different parts of the system and then applying those rates to like parts over the system as a whole. Traditionally, leakage rates from unlined canals and reservoirs are categorized just by the permeability of the surrounding soils, whereas for lined components, crack density is also considered. However, if these components are embedded in and interact with a shallow groundwater system, then the influence the system has on the loss or gain rate should also be taken into account. The goal of this study is to provide a conceptual shallow groundwater model within the plantation to better constrain how water lost from the irrigation system moves through the shallow subsurface, interacts with the irrigation system and ultimately recharges the basal aquifer. This conceptual model will aid future management decisions and provide a context for interpreting reservoir and canal seepage measurements. In a broader context, this is a case study in which geophysical methods are used in a reconnaissance mode to characterize the shallow groundwater flow system in a large-scale agricultural setting dominated by facture flow.

Study Site

The HC&S plantation extends from an elevation of 10 m above sea level in the isthmus between East Maui (Haleakala Volcano) and West Maui (Mauna Kahakawai Volcano), to over 340 m on the lower slope of the 3,055-m tall, Haleakala Volcano (Fig. 2). Haleakala Volcano and Mauna Kahakawai Volcano are shield volcanoes, the bulk of which is composed of shield- and post-shield-stage lava flows, with lesser amounts of rejuvenated-stage volcanic rocks covering the summit of Haleakala Volcano (Stearns and MacDonald, 1942). The main shield-building stage of the younger Haleakala Volcano is represented by the Honomanu Basalt, which is a thick accumulation of tholeiitic basalt flows. The Honomanu Basalt includes lava-tube-bearing, pahoehoe flows, massive aa flows and clinker beds. Honomanu flows dip at 12° at the summit of Haleakala Volcano and are near horizontal in the isthmus, where they ponded against Mauna

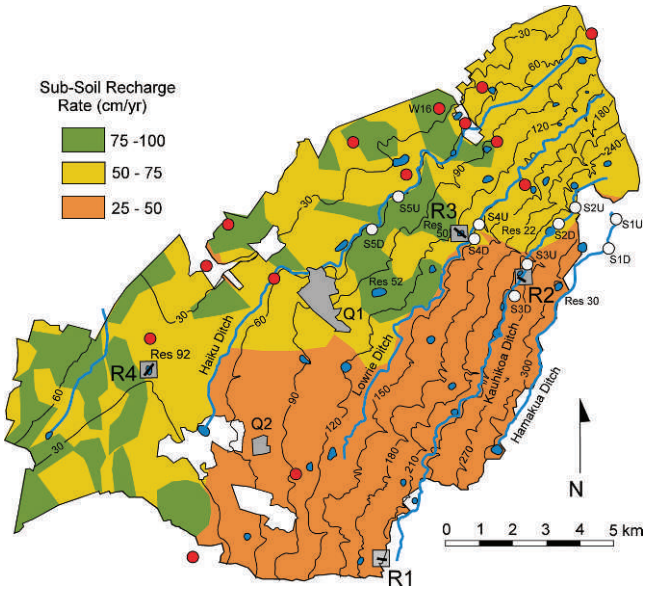

Figure 2. HC&S plantation, Maui, Hawaii. Land under cultivation is shown and corresponds to the area marked with the hash pattern in Fig. 1. Elevation contours in meters above sea level are indicated by black curves. Major irrigation water canals are indicated by blue curves. Water reservoirs used for temporary storage are indicated in blue. The location of the quarries, shown in Fig. 3, are indicated in grey. The locations of wells that produce water for irrigation from the basal aquifer are indicated by red circles. Paired up- and down-flow sites where water samples for radon analysis were collected are indicated by white circles. Sites of resistivity profiles shown in Fig. 6 are indicated in grey rectangles that correspond to the land areas shown in Fig. 6. Short black line segments within the grey rectangles indicate the location of resistivity profiles, labeled R1, R2, R3 and R4. The variation in sub-soil recharge over the plantation, predicted by Engott and Vana (2007), is shown in the color scale.

Kahakawai Volcano. The combination of lava tubes, clinker beds and fractured pahoehoe flows results in lateral hydraulic conductivities that range from 550 to 1,650 m/d (Gingerich, 1999a). The effective vertical hydraulic conductivity through the thickness of the lava flows is likely to be two orders of magnitude less, because of intervening more massive aa flows and lower vertical continuity of fractures between flows. Typically, anisotropy with ratios on the order of 200 to 1 for lateral to vertical hydraulic conductivity, are assumed for modeling purposes (Gingerich, 2008).

A volcanic hiatus occurred at the end of the Honomanu period, 0.93 million years ago, during which the Honomanu surface was eroded into incised valleys and covered by a red, ashy soil (Stearns and MacDonald, 1942). This surface was then buried by the post-shield-stage, Kula Volcanics. The Kula Volcanics are ankaramite and alkali basalt in composition and range in age from 0.36 to 0.93 million years. The unit is thickest near the summit of Haleakala Volcano, where it reaches a thickness of 600 m or more and tappers to a thickness of 40 m in the isthmus between the two volcanoes (Stearns and MacDonald, 1942). Individual flows and clinker beds of the Kula Volcanics are thicker and contain less void space than the flows of the Honomanu Basalt and are separated by numerous erosional surfaces and buried soils, particularly near the top of the formation. Hence, the contrast between the horizontal and vertical hydraulic conductivity of the Kula Volcanics is likely greater than that of the underlying Honomanu Basalt (Gingerich, 1999b). Stearns and MacDonald (1942) reported that the Kula Volcanics are weathered to saprolite to a depth of 15 m, high on the northern flank of Haleakala Volcano, where precipitation ranges between 1,200 to 1,300 mm/yr. At lower elevations, where the precipitation is less, the Kula Volcanics are significantly less weathered. This is consistent with weathering patterns observed on Oahu, Hawaii (Izuka, 1992).

Where the Kula Volcanics Formation is exposed in quarries within the HC&S plantation, the near surface consists of a 1- to 2-m thick modern soil. The soils within the plantation consist mainly of Mollisols (80%), which are moderately weathered, calcium-rich, silty-clay soils and Oxisols (15%), which are highly weathered, silty-clay soils that are rich in hydrous oxides of aluminum and iron. Both Moillisols and Oxisols are weathering products of basalt. There are also minor areas of sandy soils formed on a thin sedimentary section at the lowest elevations of the plantation. Soil hydraulic conductivities over most (80%) of the plantation ranges from 25 to 32 cm/d, with areas of 32-83 cm/d in the upper elevations and smaller areas of 94-100 cm/d in the soils formed on the sedimentary section at the lower elevations. The Mollisol and Oxisol soils grade into a variably thick saprolite layer, which typically has low hydraulic conductivities, from 2.5 to 4.0 cm/d (Wentworth, 1938), but locally can have hydraulic conductivities in excess of 80 m/d (Miller, 1988). With increasing depth, the saprolite grades into weathered, but largely intact basalt (Fig. 3). The weathered Kula Volcanics layer below the saprolite zone contains enough fresh basalt to make it worth quarrying for road metal. However, the surfaces of natural factures within the basalt are coated with clay mineraloids, such as allophane and imogolite, which form as weathering byproducts (Fig. 3(c); Wada *et al.*, 1972). When wet, these clay coatings form hydrous gels, which reduce the hydraulic conductivity (Hunt, 1996). Their presence,

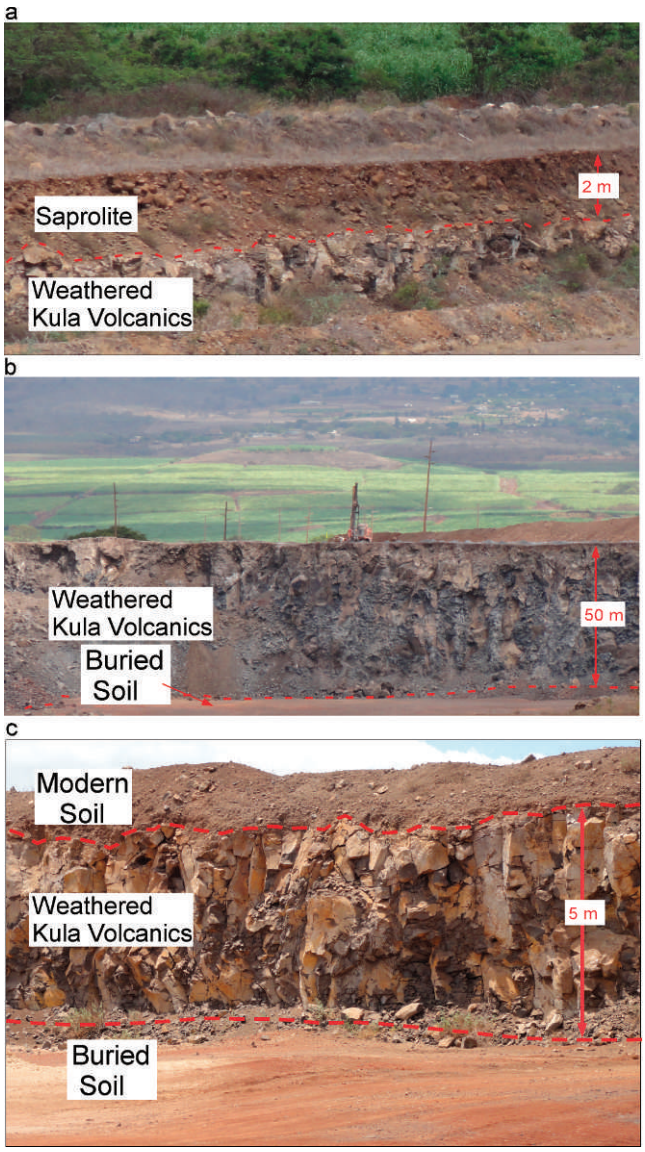

Figure 3. Exposures of the Kula Volcanics within the HC&S plantation. a) Saprolite and weathered Kula Volcanics exposed in a quarry in the central part of the plantation, labeled Q1 in Fig. 2. b) At this location there is a 2-m thick soil and saprolite layer over 50 m of Kula Volcanics, with a buried layer of red soil at its base. c) Weathered Kula Volcanics exposed in a quarry near the southwestern edge of the plantation, labeled Q2 in Fig. 2. At this location there is a 2-m thick soil layer, directly on top of 15 m of Kula Volcanic, which overlies a similar buried red soil layer. Weathering byproducts coat natural factures in the basalt.

within otherwise air-filled fractures in massive rock, would also be expected to reduce the electrical resistivity (Table 1).

Within the isthmus between East and West Maui, the Kula Volcanics are interbedded with and overlain by a thin Quaternary sedimentary sequence (Stearns and MacDonald, 1942). These deposits consist of alluvium shed from the adjacent volcanoes, calcareous marine sediments, reef deposits and both consolidated and unconsolidated dune deposits of mixed calcareous and basaltic sand. The hydraulic conductivities within the Quaternary sequence vary, but the overall range of 10 to 200 m/d is greater than that of the saprolite and weathered basalt, and significantly less than that of the unweathered basalt (Gingerich, 2008).

Table 1. Electrical resistivities of near-surface materials, Maui, Hawaii (Mattice, 1981).

Material type	Resistivity (Ohm-m)
Dry soil	170 - 800
Wet soil	10 - 100
Unsaturated saprolite	70 - 175
Saturated saprolite	25 - 120
Dry weathered basalt	1,000 - 8,000
Freshwater-bearing, weathered basalt	45 - 150
Dry basalt	2,000 - 20,000
Freshwater-saturated basalt	300 - 900
Seawater-saturated basalt	3 - 8

The hydrology of Maui is dominated by the rain-shallow effect of Haleakala Volcano (Fig. 1). Its eastern flank, which faces the Trade Winds, receives an average of 4,500 mm of precipitation per year. Long term exposure to this level of precipitation has left the eastern flank of Haleakala Volcano dissected by deeply incised valleys containing multilayered rain forests and flowing streams, which plunge over steep cliffs at the coast to form high waterfalls. Because of the high precipitation and anisotropic hydraulic conductivity, a perched water table occurs within the Kula Volcanics on the eastern flank. Water that makes it through the Kula Volcanics is expected to fall rapidly through the Honomanu Basalt to the basal water table (Gingerich, 1999b).

Precipitation rates decrease northeast-to-southwest across the western flank of Haleakala Volcano, such that at the southwest end of the isthmus the precipitation rate drops below 250 mm/yr (Fig. 1). The average precipitation within the HC&S plantation is approximately 500 mm/yr. As a result of long term semiarid conditions, the topography of the western flank of Haleakala Volcano, where the HC&S plantation is located, is much less dramatic than the that of the eastern flank. The gentle slope of the western flank is dissected by shallow gulches, which are dry except during infrequent runoff events. The natural landscape

is sparsely vegetated, mostly with scrub brush and cacti. The hydrologic system on the western flank of Haleakala Volcano is a one-tiered system. There are typically no springs flowing from the base of the Kula Volcanics, where it is exposed in quarries, indicating a wide-spread, perched water table is not present. Instead, there is only the basal freshwater lens floating on saltwater, near sea level. Hence, the local elevation is approximately equivalent to the depth to the basal aquifer within the plantation.

The tropical climate of Maui is ideal for sugarcane production. The problem faced by potential sugarcane growers of the late 1800's was that the eastern flank of Haleakala Volcano is too steep to farm and the western flank is too dry. Entrepreneurial growers solved this problem by constructing an elaborate system of hand-dug tunnels, canals and temporary storage reservoirs to convey water from streams on the eastern flank to sugarcane fields on the western flank of the volcano. Water enters the plantation through a system of four main canals or ditches that trend sub-parallel to elevation contours, north-south across the width of the plantation, at four different elevations (Fig. 2). Because of its limited interaction with the subsurface, the entering surface water is extremely fresh, typically ranging from 20 to 36 μS/cm (Table 2) or resistivities from 278 to 500 Ohm-m. The tunnels and canals are almost all concrete lined, whereas only 3 of the 43 reservoirs are lined, with the rest being unlined, earthen structures (Fig. 4). The main ditches total 70 km in length and are about 5 m wide. Water is conveyed down slope from the main ditches through smaller canals, called chutes, to the reservoirs and from there on to the fields. There are 190 km of chutes, which average about 2.4 m in width. The ditch water is augmented by water pumped from 15 hand-dug wells that extend to the basal water table near sea level. Because of its interaction with seawater below the fresh lens, the well water is brackish, with conductivities ranging from 1,000 to 3,000 μS/cm or resistivities between 3.3 to 10 Ohm-m.

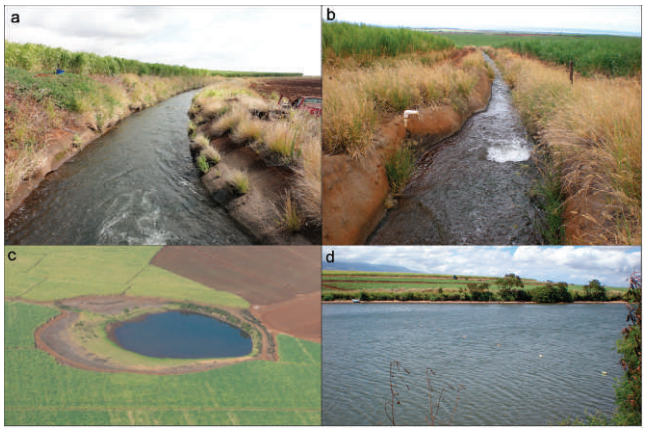

Figure 4. Irrigation conveyance elements within the HC&S plantation. a) Example of the 70 km of major supply canals or ditches, which are 5 m wide and flow sub-perpendicular to slope. b) Example of the 190 km of smaller canals or chutes that carry water from the ditches, down slope to the reservoirs. c) Example of the 43 small reservoirs used for temporary storage, which typically have surface areas of 2 to 3 hectares. d) Reservoir 50, viewed from the down-slope dam, looking west, up the flank of Haleakala Volcano. Floats supporting the 28-electrode marine array used to cross the reservoir are visible in the foreground.

Until the mid-1970s, water was applied onto the fields by furrow irrigation. The efficiency of furrow irrigation on the HC&S plantation was thought to be about 50%, meaning that half of the water applied to the fields was taken up by the crop and the other half was lost through a combination of evaporation from the furrows and infiltration past the root zone. The water that infiltrated past the root zone was thought to ultimately recharge the basal aquifer (Engott, 2006;

Table 2. The values of radon (^{222}Rn) activity (Bq/m^3) and conductivity (μS/cm) are shown for up- and down-flow water sampling locations with associated named ditches. One sample standard deviation for four radon measurements at each station is given in parenthesis. Approximate age of sugarcane is shown in years. The n.a. abbreviation stands for not applicable because the upslope field was covered by an exotic grass.

		Radon (Bq/m^3)		Conductivity (μS/cm)		
Sample	Ditch	Up flow	Down flow	Up flow	Down flow	Approximate Sugarcane Age (yrs)
1	Hamakua	142 (±54)	0 (±0)	20	35	n.a.
2	Kauhihoka	0 (±0)	170 (±33)	35	36	2.0
3	Kauhihoka	0 (±0)	28 (±28)	27	28	1.0
4	Lowrie	85 (±28)	28 (±28)	1,042	1,042	0.3
5	Haiku	114 (±46)	142 (±54)	1,170	1,517	2.0

Engott and Vana, 2007). Today, the irrigation water is applied by subsurface drip irrigation, which is thought to be about 80 to 95% efficient (Izuka *et al*., 2005). Hence, the switch from furrow to more efficient drip irrigation was accompanied by a marked decrease in recharge of the basal groundwater system (Engott, 2006).

The changeover to drip irrigation was complete by the mid-1980s. Since that time, all of the 183 separate fields that make up the HC&S plantation have been managed in the same way. Local weather conditions are continuously monitored throughout the plantation. This information is used to adjust the amount of irrigation water applied to each field on a daily basis to augment precipitation, such that the total water received matches the amount lost by evapotranspiration (ET) divided by the estimated efficiency with which the crop takes up the water. Potential ET varies over the plantation from 180-200 cm/yr in the upper elevations of the plantation to 230-250 cm/yr in the lower elevations (Engott and Vanba, 2007). Hence, more irrigation water is required to match ET in the lower elevations of the plantation than the upper elevations.

The sugarcane is grown and harvested field-by-field in a two-year cycle, such that somewhere on the plantation a field is being planted and another is being harvested, on a nearly continuous basis. The sugarcane is planted throughout the plantation as seed stalks spaced approximately 1-m apart in rows approximately 2-m apart. A new drip system is installed in each field prior to planting. For the first few months after planting, the root system has not sufficiently developed to use all the water being applied. Hence, more water would be expected to bypass the root zone in young sugarcane compared to sugarcane that is a year old or more. Then, during the final months prior to harvest, watering is gradually reduced over a 40-day period and then withheld entirely for the last two months before harvest to force the sugarcane to store the maximum amount of sugar. From the beginning of this pre-harvest ripening period to after the field has been harvested and replanted, the only water reaching the fields involved is from precipitation. Hence, little or no water would be expected to pass through the soil during the ripening and pre-planting period. The variation in the rate of water uptake of the sugarcane during its life cycle means that the rate at which irrigation water infiltrates below the root zone also varies with the local age of the sugarcane throughout the plantation. Because the measurements made in this study are sensitive to moisture levels and flow rates below the root zone, we record the approximate age of the sugarcane at each location measurements are made.

From 2003 to 2011, precipitation within the HC&S plantation averaged 226,100 m^3/d and the total inflow to the irrigation system during that period averaged 713,900 m^3/d. From 1 to 2% of the inflow is expected to be lost because of evaporation from the canals and reservoirs; most of the rest is applied to the fields. However, a significant, but poorly constrained, fraction seeps from the canals and reservoirs into the shallow subsurface before reaching the fields. Loss rates in 31 of the 43 reservoirs on the HC&S plantation were measured in the 1960s using ponding-test methods similar to those used by Ham and Baum (2009). At that time, the average loss rate from the reservoirs ranged from 12 to 15 cm/d. Until the 1960s, it was standard practice to periodically drain the reservoirs and remove the accumulated sediment. However, repeat ponding tests before and after cleaning of the reservoirs indicated that the cleaning process caused the leakage rate to increase. Hence, after the 1960s, the practice of periodically cleaning the reservoirs was abandoned. Repeat ponding measurements in 2013 in four reservoirs showed a 70% drop in the seepage rate from the 1960s, to the range of 3 to 5 cm/d. The first ever seepage measurements in HC&S canals were also made in 2013. Two segments that span the range of canal conditions from mostly intact to average condition were tested using static ponding methods similar to those used to test the reservoirs, producing loss rates of 6 and 12 cm/d. Hence, the lined canal segments that have been tested tended to leak more than the recently tested unlined reservoirs.

The working hydrologic model used to estimate recharge to the East Maui basal aquifer (Gingerich, 1999b; Engott and Vana, 2007) is that water from irrigated fields that infiltrates beyond the 60-cm root depth of the sugarcane moves vertically to the basal groundwater table near sea level. The amount of water entering the sub-soil zone is a function of the hydraulic properties of the soil, meteorological variations over the plantation, irrigation practices and the efficiency of water uptake by the crop, all of which are known with varying degrees of uncertainty. Historically, two approaches have been used to account for the contribution of irrigation to recharge on Maui. The method used by Shade (1976, 1997) for West Maui relies on measurements of the total water supplied to plantations. The total inflow is discounted for leakage and evaporation within the conveyance system and the remainder is assumed to be applied uniformly to the fields. Precipitation minus runoff is added, ET is subtracted and the resulting soil moisture is tracked over time. The recharge over time is then assumed to be given by the excess moisture beyond the soil zone storage capacity. Because this method does not account for spatial differences in water application rates, it tends to predict less recharge in areas of high ET.

The method used by Engott and Vana (2007) to compute recharge differs from Shade (1996, 1997) in

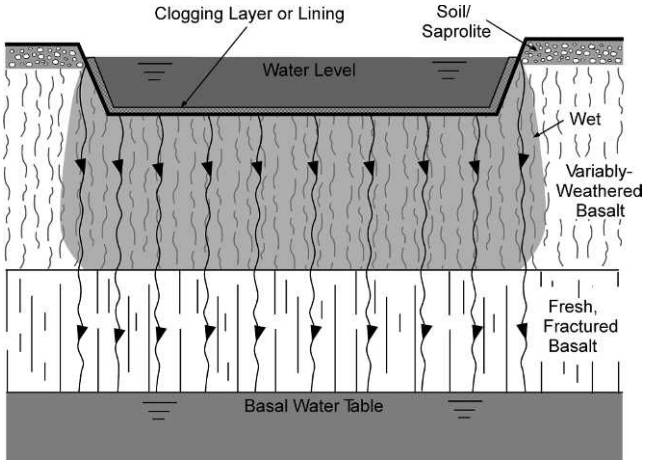

Figure 5. Initial conceptual model of vertical infiltration and recharge from a surface water body, well above the water table. Modified from a more general model proposed by Bouwer (2002). Within the HC&S plantation, a 1- to 2-m thick soil and saprolite layer overlies variably weathered basalt containing buried soil layers, which in turn overlies relatively unweathered fractured basalt. In this model, water flows vertically from irrigation canals and reservoirs, through the weathered basalt interval over a period of months or years and then falls through the underlying fractured basalt to the basal water table in days.

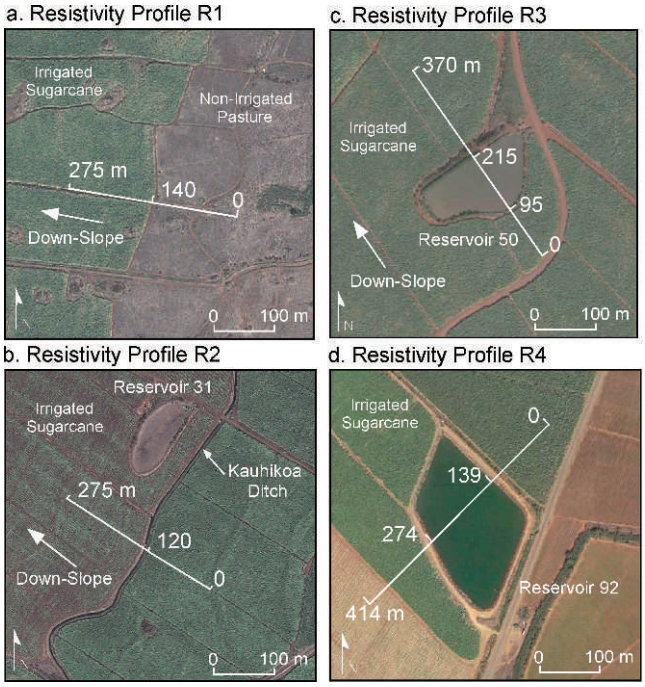

Figure 6. Settings of resistivity profiles. a) Resistivity profile R1 extends from non-irrigated pasture land up slope of the plantation, down slope into irrigated sugarcane. b) Resistivity profile R2 begins down slope of irrigated sugarcane, and extends through irrigated sugarcane across a canal and through a recently harvested sugarcane field. c) Resistivity profile R3 begins down slope of irrigated sugarcane at mid-slope, and extends across a reservoir and into more irrigated sugarcane down slope of the reservoir. d) Resistivity profile R4 is located in the isthmus between East and West Maui, near the saddle point, and is parallel to the axis of the isthmus. It extends from irrigated sugarcane, across Reservoir 92 and extends through more irrigated sugarcane. The aerial photographs were not taken at the time of the resistivity surveys. Hence, the sugarcane age shown in the photographs is not indicative of the sugarcane age during the surveys.

that it accounts for the irrigation practices followed on the HC&S plantation. Engott and Vana (2007) assumed that over most of the plantation the supply of irrigation water was always sufficient to match ET, plus an additional 25% to account for the estimated 80% efficiency of the drip system. However, in the fields upslope of Lowrie Ditch there is typically insufficient water available to meet this demand. Engott and Vana (2007) accounted for this short fall by reducing the amount applied by multiplying the target amount by a constant 0.8 factor. The estimated recharge over time was then assumed to be 20% of the total water received by each field. As a result, this method predicts more recharge in areas of high ET (Fig. 2).

All of the water that makes it to the base of the soil is expected to infiltrate slowly through the sub-soil weathered zone because of its relatively low hydrologic conductivity, and then fall rapidly to the basal groundwater table once it reaches the unweathered basalt (Fig. 5). If the seepage water moves in this way, one would expect anomalously low resistivities within the weathered zone directly beneath irrigated fields, canals and reservoirs. Furthermore, the amplitude and vertical extent of the resistivity anomalies would be expected to correlate with local seepage rates, with low resistivities extending to greater depths beneath zones of higher seepage. The key assumption in this model is that the infiltration water drains efficiently to the basal water table, such that there is no two-way interaction between the ground water and the surface water. One of the main objectives of this study was to determine if the water movement within the shallow subsurface beneath the HC&S plantation is consistent with this working hydrologic model.

Methods

In many cases, shallow groundwater systems at the farm to regional scale can be characterized reasonably well by discrete sampling and monitoring in boreholes (*e.g.*, Bosch *et al.*, 2003; Priest, 2004; Dewandel *et al.*,

2008). However, systems that are dominated by facture flow, as is the case for subsoil-flow on Maui, are notoriously difficult to characterize by discrete sampling (Biggar and Nielsen, 1976; Baker, 2006; Brown *et al*., 2011). Fractures offer fast pathways by which most of the flow occurs and yet the factures are difficult if not impossible to characterize in terms of their effect on the bulk hydraulic properties from borehole samples (Kung *et al*., 1991). The bulk hydraulic properties of a fractured rock volume are not only influenced by the number and size of fractures, but the degree of interconnectivity between fractures. Wood *et al*. (2000) summarized the problems involved in characterizing fracture flow systems and suggests possible solutions. Geophysical and radiometric methods were listed as potentially useful because they respond to average properties over significant rock volumes. In this study, we use direct current resistivity profiling as the primary tool for identifying flow pathways in the shallow subsurface. Because validation of the resistivity results by discrete subsurface sampling is problematic in fracture flow systems, we measured Radon (^{222}Rn) levels in surface water and well water to seek corroborating evidence for interaction between the shallow ground water and the irrigation systems within the HC&S plantation.

DC Resistivity Profiling

Prior electrical resistivity investigations on Maui have established the resistivity ranges for dry and wet near-surface materials, and suggest that DC resistivity profiling would be useful for characterizing the shallow flow systems (Table 1). In the natural state, in which the western flank of Haleakala Volcano is nearly dry down to the basal water table near sea level most of the time, resistivities should range from 170 to 800 Ohm-m in the dry soil zone, 70 to 175 Ohm-m in dry saprolite, 1,000 to 8,000 Ohm-m in the dry, weathered basalt and 2,000 to 20,000 Ohm-m in the dry, unweathered basalt (Mattice, 1981). Regions in which these zones have been invaded by moisture from the irrigation system should have significantly lower resistivities. Hence, if the vertical infiltration model is correct, we would expect to see anomalously low resistivity zones beneath irrigated fields and potentially thicker low-resistivity zones beneath the canals and reservoirs.

The dimensions of the HC&S plantation average about 12 km from the base of Haleakala Volcano to the upper elevations of the plantation and about 12 km perpendicular to slope. In spite of its size, there are relatively few suitable sites to collect long resistivity profiles. Sugarcane stands older than a few months are too dense to penetrate on foot, and cutting a path with heavy equipment would damage the drip irrigation system. Hence, resistivity data collection is limited to recently harvested fields, planted fields only a few months old and the unpaved roads that separate individual fields. To characterize the near-surface moisture distribution within the plantation and how it is influenced by irrigation, we selected four profiles that are 260 to 400 m in length and oriented parallel to slope (Fig. 2). We chose the profiles to characterize the transition from dry, non-irrigated land, upslope of the plantation, to irrigated sugarcane fields progressively further down slope, to the axis of the isthmus. The profiles also cross a main canal and two reservoirs. In each case, the profiles are placed to straddle the main hydrologic feature being tested, with the half of the profile up-slope of the feature serving as the control for the other half down slope of the feature. If the profile segments upslope, down slope and beneath a particular feature show the same resistivity pattern, then the feature would be interpreted as having no effect on the sub-soil flow system.

In addition to the main elements of the irrigation system, the profiles where chosen to characterize the influence of other potential hydrologically important variables on sub-soil flow. Topographically, the profiles range from an elevation 32 m above sea level, with an average slope of 0.3° in the isthmus, to 280 m above sea level, with an average slope of 16.5°. Profiles 1 and 4 are in the drier, southern part of the plantation, whereas Profiles 2 and 3 are in the wetter, northern part of the plantation (Fig. 1). Profiles 1, 2 and 3 are in the dominant Mollisol soils with hydraulic conductivities in the range of 25 to 32 cm/d, whereas Profile 4 samples the zone of sandy soils with the highest hydraulic conductivities (100-300 cm/d) in the isthmus. Profiles 1 and 2 are in the region above Lowrie Ditch, with the lowest rate of recharge into the sub-soil zone predicted by Engott and Vana (2007; Fig. 2). Profiles 3 and 4 are located in regions Engott and Vana (2007) predicted intermediate rates of sub-soil flow (Fig. 2). Taken together, these profiles sample the range of hydrologic settings within the plantation and characterize how these settings differ from the natural state of non-cropped land outside of the plantation.

The resistivity profiles were collected with a 56-electrode, 8-channel, AGI SwiftSting R8^{TM} resistivity instrument, using an electrode spacing of 5 m and roll-along, dipole-dipole acquisition. Resistivity profile R1 began in a fallow field that had not been irrigated for 8 years and had no irrigated fields upslope. R1 continued down slope into nearly mature, irrigated sugarcane. Resistivity profile R2 began down slope of irrigated sugarcane, continued through nearly mature, irrigated sugarcane, crossed a main canal and extended into a harvested field that had been recently irrigated, but was not being irrigated at the time of the survey. The canal crossing was accomplished by positioning the

profile such that one electrode was centered in the canal crossing and was left inactive during recording. Resistivity profile R3 was located down slope of R2. It began in young, irrigated sugarcane, extended across the 1.25 hectare Reservoir 50 and into a young sugarcane field down slope of the reservoir. Reservoir 50 was one of those for which the leakage rate was measured in the 1960s and again in 2013. Resistivity profile R4 began in young, irrigated sugarcane, extended across the 2.9 hectare Reservoir 92 and into more mature sugarcane at the base of the plantation, along the axis of the isthmus.

The reservoir crossings were accomplished by first placing the instrument on the upslope shore of the reservoir, connecting a 28-electrode land cable to the low-electrode-number side of the instrument and extending it upslope and connecting a 28-electrode marine cable with 5-m electrode spacing to the high-electrode-number side of the instrument. The marine cable was supported on the reservoir surface by floats along its length and stretched across the reservoir to its down-slope shore (Fig. 4(d)). Once this profile segment was recorded, the instrument was moved to the opposite shore. The marine cable was reversed in orientation, laid back along the same line and connected to the low-electrode-number side of the instrument. The 28-electrode land cable was then connected to the high-electrode side of the instrument and extended over the reservoir dam and down-slope into the sugarcane field beyond. This procedure resulted in unbroken data collection across the reservoirs, with source electrodes on land and receiver electrodes in the water and vice versa on both sides of the reservoirs.

The marine resistivity cable used in the water-crossing segments differs from a normal land resistivity cable in that it contains a layer of water-blocking tape beneath the outer jacket that prevents the lateral movement of any water that might enter the cable either through small holes in the jacket or around the electrode moldings. Submerging resistivity cables that lack such a water-blocking layer may permanently damage the cables (AGI, 2006). In a side-by-side comparison on land, between the marine cable and the land cables used in this study, the marine cable produced apparent resistivity values that were approximately 3% higher than those recorded with the land cables. This offset was likely caused by the higher contact resistance of the graphite electrodes used in the marine cable. The offset was similar in magnitude to the noise levels within the data collected on the land-only segments. Hence, the error introduced by using the different types of cables on the land and water segments was deemed acceptable for the purposes of this study.

Combining resistivity data collected on land and over water in the same data set is not novel to this study. A similar approach was used to assess the exchange between ground water and natural lakes by Engesgaard *et al*. (2010), Rosenberry *et al*. (2010) and Toran *et al.* (2010), and in coastal-marine environments by Swarzenski and Izbicki (2009) and Apostolopoulos (2012). These prior studies involved profiles straddling a single shore line, with one land segment and one water segment. This study differs from these prior studies in that it involves crossing water bodies, with land segments to either side of a water segment.

There are a number of potential problems in combining land and water segments in the same resistivity data set. If the water is moving rapidly, flow over the electrodes could produce so-called streaming potentials. For marine shorelines, the potentially large contrast in resistivity between the seawater (0.25 Ohm-m) and land can cause problems. There are also special features built into commercial resistivity inversion programs that treat water segments differently than land segments. However, in this study, water in the small reservoirs crossed is calm, the water is fresh (10 to 50 Ohm-m) and no special treatment was applied to the water segments during inversion. Hence, none of the most common problems in combining land and water resistivity surveys factored into this study.

The resistivity profiles were inverted using AGI EarthImager2D^{TM}. Elevation change along the profiles, as well as relief on manmade features, such as the canal and reservoir dams, influences the resistivity response. To account for topographic effects, the elevations of the electrodes were determined by land surveying methods and incorporated into the resistivity data inversion process. For both the canal and reservoir crossings, the water surface was taken as the upper surface of the model and the water and any concrete lining or sediment within the reservoirs were treated as variable resistivity regions within the model. Data collected in sugarcane fields under active irrigation showed high spatial variability, but the measurement repeatability error was generally less than 3%. Rather than using small finite elements throughout in an attempt to fit this variability, we used 2.5-m wide elements and a smoothness constrained solution, with the objective of minimizing the L2 Norm rather than the RMS error; this places less weight on outlier measurements. All profiles converged to a L2 Norm below 1.0, but the residual root-mean-square difference between the forward model response and the measurements remained between 10 to 20% in some cases because of misfit within the shallow subsurface of the irrigated fields.

Radon Measurements

Resistivity profiling can reveal subsurface moisture patterns, but it is a not a direct indicator of flow.

To directly test for groundwater/surface interaction, we measured radon levels in reservoirs, canals, the inflow of surface water from East Maui and in a representative supply well in the basal aquifer. Isotopic radon (^{222}Rn), with a half-life of 3.8 d, is produced as a daughter product of radium decay. Radon is present in ground water that has been exposed to uranium bearing rocks for a length of time prior to sampling and is generally not present in detectable amounts in surface water (Corbett *et al*., 1997). Hence, detection of radon can be used as a tracer of groundwater inputs into surface water and to locate the entry points or zones of the groundwater contribution to surface water (Cook *et al*., 2003, 2006; Cook, 2012; Mullinger *et al*., 2007; Burnett *et al*., 2010). Surface water entering the HC&S plantation is expected to lack detectable radon because of its limited exposure to uranium-bearing rocks in rapid transit from the eastern flank of Haleakala Volcano. The presence of radon in detectable amounts within the plantation could only occur as the result of addition of well water to the surface water or by infiltration of shallow ground water into canals and reservoirs through their sides and bottoms. Therefore, any increase in radon levels in the down-flow direction within the canals without an intervening well-water input point would indicate infiltration of ground water into the canal. Similarly, radon levels within reservoirs that are higher than levels within the supplying canal would indicate infiltration of ground water into the reservoir. However, seepage from canals and reservoirs would not influence the radon concentration.

We tested for groundwater gain by collecting water samples from representative reservoirs and canal segments. The water samples were collected by immersing 250 ml glass bottles 10 cm below the water surface to avoid contact with the atmosphere. The bottles were sealed underwater using Teflon lined caps, insulated and returned to the laboratory for ^{222}Rn activity measurements. Samples were analyzed within about 4 hours of collection to minimize the loss of radon caused by radioactive decay. For each sample, dissolved ^{222}Rn was measured using the RAD7 (Durridge Inc. Billerica), equipped with a water probe and a RAD7H2O radon-in-water grab sample accessory. Prior to each measurement, the RAD7 was purged for a minimum of 30 minutes to reduce contamination of samples from ambient radon. In addition, a blank sample composed of distilled water was tested before each sample run.

To assess potential down-slope-directed flow interception of shallow ground water by reservoirs, water samples were collected from Reservoirs 22, 30 and 52 on December 16-17, 2013. Reservoirs 22 and 30 were only supplied by surface water. Hence, any radon detected in these reservoirs would to be from groundwater sources. Reservoir 52 was supplied by a combination of surface water and well water, with radon potentially being derived from both sources. For Reservoirs 22 and 30, water samples were acquired from the main canal gate, where the water leaves the canal and enters the chute to the reservoir, the middle of the inflow chute leading to the reservoir and two samples within the body of the reservoir.

Canal interception of shallow, down-slope-directed groundwater flow was assessed by sampling water from the four main canals, Hamakua, Kauhihoka, Lowrie and Haiku, during December 18-19, 2013. These canals were chosen to represent the topographic gradient, with the Hamakua Ditch at the highest elevation of 340 m and the Haiku Ditch at the lowest elevation of 34 m above mean sea level. Water samples were collected from the canals at up- and down-flow locations adjacent to sugarcane fields, with sampling locations separated by an average distance of 800 m. For these paired measurements, increase in radon concentration in the flow direction would be evidence for groundwater infiltration into the canal. The electrical conductivity of the water was measured at each sample location at the time of sample collection to identify the source of the water. Waters with electrical conductivities less than 100 μS/cm were interpreted to be surface water from East Maui, whereas waters with electrical conductivity greater than 1,000 μS/cm were interpreted to contain a significant well-water component. Five pairs of water samples were collected in total, with two samples collected at different locations along the Kauhihoka Ditch.

Water samples were also collected from water leaving the underground conduit that supplies the Kauhihoka Ditch and from a 7.7-m deep, hand-dug well near the base of the slope, referred to as Well 16. The water from the underground conduit was used to assess the potential addition of radon to surface water flowing in the conduit from surrounding basalt rocks. The water from Well 16 was collected as a reference of groundwater radon concentration amounts in the basal aquifer.

Results

Resistivity Profiling Results

The inverted resistivity section for profile R1 shows resistivities up to 5,000 Ohm-m at the ground surface and extending to a depth of 5 to 10 m in the non-irrigated segment (Fig. 7(a)). This is consistent with the resistivity of dry, weathered basalt, but is higher than expected for dry soil from Table 1. The high resistivities could be caused by extremely low moisture levels. Below that depth, resistivities are shown to decrease to the 50 to 250 Ohm-m range. This range overlaps that expected for dry soil and dry, weathered saprolite. It is also possible that the apparent decrease in resistivity could be an inversion artifact associated with measurement error

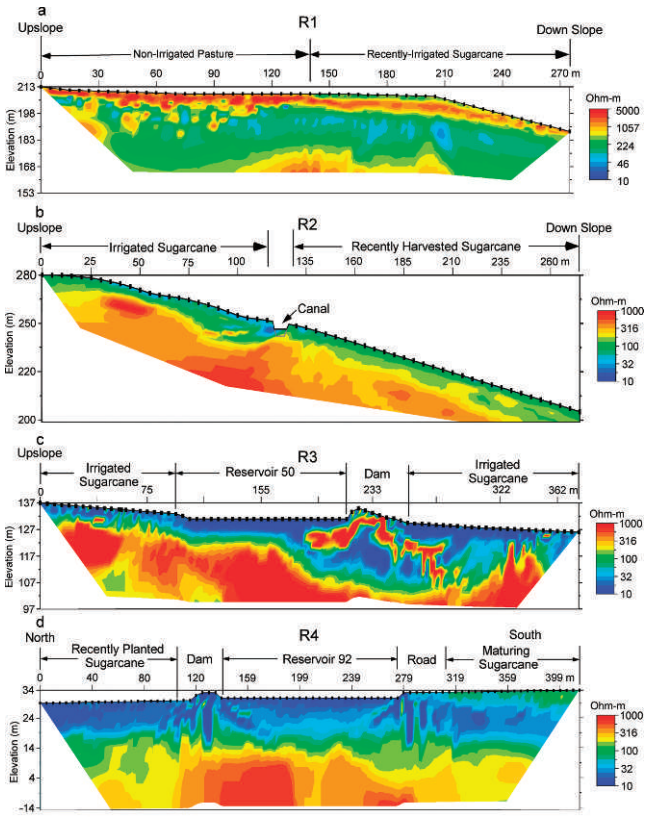

Figure 7. Resistivity profiles in different hydrographic settings. All profiles are oriented parallel to topographic slope. a) Resitivity profile R1, from non-irrigated pasture land that was last irrigated in 2005, down slope into irrigated sugarcane. b) Resistivity profile R2 extends down slope through irrigated sugarcane, across the Kauhilkoa irrigation ditch (marked "Canal") and on into a recently harvested sugarcane field. The location of the concrete lining of the canal bottom is outlined in grey to show its location, but was not specified in the inversion process. c) R3 extends further down slope through irrigated sugarcane, across Reservoir 50 and into another irrigated sugarcane field below the reservoir. d) R4, located near the saddle point in the isthmus between East and West Maui, begins in recently planted sugarcane, crosses Reservoir 92, and extends across more mature, irrigated sugarcane. The locations of the profile within the HC&S plantation are shown in Fig. 2. The horizontal and vertical spatial scales differ between the four profiles and the resistivity scale used in part (a) differs from that used in parts (b), (c) and (d). The scales in each case were chosen to best show the features of the individual sections.

caused by the high electrode contact resistance in the dry soil (1,000 to 1,200 Ohm) or limited model sensitivity below the extremely high-resistivity upper layer. Starting at the upslope edge of sugarcane approximately 18 months of age, there is a surficial, low-resistivity layer (~250 Ohm-m) extending from the surface to depths of 1 to 2 m.

The upslope end of resistivity profile R2 is within sugarcane approximately 12 months in age and is also down slope of irrigated sugarcane (Fig. 7(b)). It shows a surficial, low-resistivity layer similar to that on profile R1. However, the low-resistivity layer on profile R2 is thicker (10 to 15 m) and lower in resistivity (32 to 100 Ohm-m). The low-resistivity layer extends below the soil and into weathered Kula Volcanics. It thickens to approximately 20 m and becomes less resistive (10 to 32 Ohm-m) upslope of the canal crossing. The low-resistivity layer then reverts back to a thickness of 10 to 15 m and increases in resistivity to between 32 and 100 Ohm-m down slope of the canal crossing and across a field that had been harvested within the previous month.

Resistivity profile R3, which is located down slope of profile R2, begins in approximately 2-month old sugarcane (Fig. 7(c)). It shows an even more well developed surficial low-resistivity layer (10 to 20 Ohm-m) at the upslope end of the profile, which increases in thickness and decreases in resistivity as the profile crosses Reservoir 50 (Fig. 6(c)). Resistivities up to 1,000 Ohm-m below the low resistivity layer are consistent with dry, weathered basalt. Most of the reservoir is underlain by a relatively thin low-resistivity layer. However, in a 15-m wide zone about three-quarters of the way across the reservoir, the low-resistivity layer arches down to a depth of 25 m, curves beneath the dam and beneath the approximately 3-month old sugarcane down slope of the dam.

Resistivity profile R4 is located in the lower elevations of the plantation, along the axis of isthmus, approximately in the middle of the isthmus (Fig. 2). The profile begins in sugarcane less than 1-month old, crosses Reservoir 92 and continues across approximately 6-month old sugarcane. A surficial resistivity layer is also present on profile R4 (Fig. 7(d)). However, on this profile, the low-resistivity layer is essentially uniform in thickness (15 to 20 m) and resistivity (10 to 32 Ohm-m) across both sugarcane fields and Reservoir 92. However, within the low-resistivity layer, there is a thin, relatively high resistivity, surficial layer (1 to 5 m; 100 Ohm-m) beneath the more mature sugarcane on the southern third of the profile. Relative to profiles R1, R2 and R3, which are all on the lower slope of Haleakala Volcano, the high-resistivity region below the low-resistivity layer on profile R4 is less resistive, with much of the zone ranging between 100 and 316 Ohm-m. Although the inverted resistivity profile is displayed to a depth of 14-m below sea level, there is no evidence of the basal water table, which should produce a lower resistivity interval below an elevation of 1 m. The lack of a response to the water table indicates model insensitivity below an elevation of 1 m.

Radon Sampling Results

Source water from the canals entering each of the reservoirs contained radon with values of 155, 117 and 39 Becquerels per cubic meter (Bq/m^3) for Reservoirs 22, 30 and 52, respectively. Water in the chute inflow for Reservoirs 22 and 30 had lower radon activity than the source canal water with values of 78 and 39 Bq/m^3, respectively. The median values of water samples collected in Reservoirs 22 and 30 were both equal to 19 Bq/m^3, a value we consider to be the detection limit of the methodology we used to measure ^{222}Rn activity. For Reservoir 52, a single water sample of water within the reservoir was found to have a radon value of 38.9 Bq/m^3, similar to the canal water supplying this reservoir.

Electrical conductivities of canal water samples indicate that at the time of sampling, Hamakua and Kauhoka Ditches contained surface water from East Maui, whereas there was a significant contribution of well water in Lowrie and Haiku Ditches (Table 2). Most of the canal sampling locations showed a difference in radon activity within water up- and down-flow of the sampling site. The one exception was site S3, the second sampling location along the Kauhihoka Ditch, which had no detected radon activity at the up- and down-flow positions (Fig. 2; Table 2). These two samples bracket the canal crossing point of resistivity profile R2 (Fig. 7(b)) and indicate no groundwater contribution to the canal along that segment. In contrast, sites S2 and S5 had higher radon activity at the down-flow position, which were sampled in the Kauhihoka and Haiku Ditches, respectively. Both of these sites had sugarcane that was approximately two years of age at the time of the sampling. The S2 sampling pair, on the northern end of the Kauhioka Ditch, showed no detectable radon at the up-flow position and a level of 155 Bq/m^3 at the down-flow position, which was the highest radon level observed in the study. The electrical conductivity of the water at the up-flow and down-flow positions was essentially the same (35 and 36 μS/cm), suggesting that any water gain was either small or of the same electrical conductivity. The S5 sample pair showed a less dramatic increase in radon (39 to 78 Bq/m^3; Table 2) and also showed a marked increase in electrical conductivity from the up-flow to down-flow positions (1,170 to 1,517 μS/cm). This indicates that higher conductivity water was being added to the canal between the two sample points, which could explain the increase in radon, down flow. However, the source of the water would have a long chute from the Lowrie Ditch, upslope of the Haidu ditch. Radon should have dropped below the detectable limit because of degassing during this long run. Sites S1 and S4 sampled along the Hamakua and Lowrie Ditches, respectively, showed lower radon activity down-flow than up-flow. The field upslope of the Hamakua Ditch sampling location was covered in non-native guinea grass (*Panicum maximum*), whereas the field upslope of the Lowrie Ditch contained sugarcane approximately 3 months of age. No radon activity was detected for water sampled from the underground conduit providing water for the Kauhihoka Ditch. The radon activity for Well 16 was 117 Bq/m^3. Hence, the surface water coming into the plantation from the east side of Haleakala Volcano contained no detectable radon, whereas the water from a representative well in the basal aquifer did contain radon.

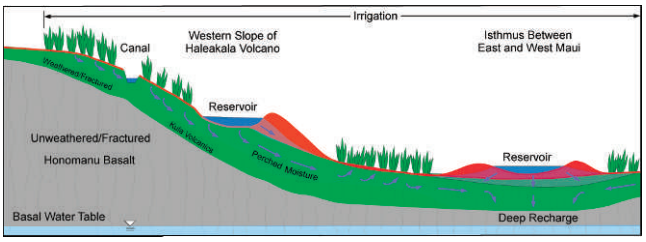

Figure 8. Conceptual model of shallow hydrology of HC&S plantation. Water that infiltrates below the soil zone moves down slope as variably saturated flow, through the weathered Kula Volcanics. The perched system thickens and becomes more saturated down slope as a result of additional water from irrigated fields and water reservoirs. Pressure head within this shallow flow system may locally reduce seepage from canals and reservoirs or even result in gain. Some amount of vertical recharge to the basal aquifer likely occurs throughout. However, recharge is concentrated in the isthmus between East and West Maui.

Discussion

The main feature observed on the four resistivity profiles is a low-resistivity layer that begins at the upslope edge of irrigated sugarcane and grows in thickness down slope to the isthmus. We interpret this low-resistivity layer as a variably-saturated layer within the weathered Kula Volcanics that is fed by irrigation water that has bypassed the sugarcane root zone and locally by seepage from reservoirs and canals (Fig. 8). By itself, the existence of a superficial, wet layer beneath irrigated crops is not surprising (Minsley *et al.*, 2010). The fact that the layer generally thickens and appears to become more saturated down slope is consistent with the predicted variation in sub-soil flow of Engott and Vana (2007), a result of the increased availability of irrigation water down-slope of Lowrie Ditch (Fig. 2). However, some of the details of the resistivity profiles cannot be fully explained by vertical recharge models proposed either by Shade (1997) or Engott and Vana (2007). Profiles 1 and 2 both occur above Lowrie Ditch in the

zone with the lowest recharge rate predicted by Engott and Vana (2007). Both profiles are in the region of Mollisol soils, with the same range of hydraulic properties. Hence, the recharge models by both Shade (1997) and Engott and Vana (2007) would predict the same rates of recharge beneath the two profiles. However, Profile 2 has a low-resistivity layer that is lower in resistivity and two to three times thicker than Profile 1 (Fig. 7(a)-(b)). The land crossed by the two profiles differ in that Profile 2 is at a higher elevation and therefore higher above the basal water table and steeper than Profile 1. Profile 2 has a top elevation of 280 m and an average slope of 16.5°, compared to a top elevation of 213 m and an average slope of 5.2° for Profile 1. Although the overall pattern between the four profiles is one of increasing thickness of the low-resistivity layer with decreasing elevation and slope, the opposite is true for Profiles 1 and 2. Hence, topographic effects alone cannot explain the sub-soil moisture distribution beneath the plantation.

Another way in which Profiles 1 and 2 differ is that Profile 2 is situated down slope of other irrigated sugarcane fields, whereas Profile 1 is down slope of a non-irrigated pasture. We suggest that the increased thickness of the apparent wet layer beneath Profile 2 compared to Profile 1 is the result of down-slope flow from the irrigated fields above Profile 2. A component of down-slope flow is also suggested by the marked increase in the thickness, up slope of a Kauhihoka Ditch, suggesting that the ditch acts as an obstruction, retarding down-slope flow. Even more striking evidence for sub-soil down-slope flow can be seen in the resistivity pattern beneath Reservoir 50, on Profile 3 (Fig. 7(c)). The low-resistivity zone on Profile 3 is 10-m thick across the upslope half of the profile. In the middle of the profile there is a 15-m wide zone in which seepage water from Reservoir 50 appears to flow vertically downward through the reservoir bottom, turn down slope, pass under the dam and then up under the sugarcane field beyond. This pattern indicates that recharge is not vertical. The flow likely occurs within a few discrete pathways distributed within the low-resistivity zone that appears on the resistivity profile. This is the nature of facture flow systems; nearly all of the flow occurs along a few fast pathways that are difficult to find by discrete sampling.

The other pattern seen in the resistivity profiles is a decrease in resistivity within the low-resistivity layer down slope (Fig. 7). Unlike the gradual increase in the thickness of the low resistivity layer, the decrease in resistivity is abrupt between Profiles 2 and 3. On Profiles 1 and 2, which receive irrigation water from the Hamakua and Kauhikoa Ditches, the low-resistivity layer is in the range of a few hundred Ohm-m. These ditches are fed only by surface water from the east side of Haleakala Volcano, which has electrical conductivity values in the range of a few 10s of μS/cm (Table 2). The marked down-slope decrease in resistivity within the low resistivity layer correlates with an increase in the electrical conductivity within the Lowrie and Hakiku Ditches that supply the fields at lower elevations (Fig. 2, Table 2). These two canals are partially sourced from well water. The occurrence of resistivities as low as 10 Ohm-m in the shallow subsurface beneath fields at the lower elevations of the plantation (Fig. 7(c)-(d)) suggests increased soil salinity, which argues against increased reliance on ground water for irrigation.

As in the case of the natural perched groundwater system on the eastern flank of Haleakala Volcano described by Gingerich (1999b), the highly anisotropic hydraulic conductivity of the Kula Volcanics is likely a major factor in the development of this anthropogenic perched system (Ginerich, 2008). Perched zones of unsaturated and saturated water in basalt terrains have been reported before on the other Hawaiian Islands and elsewhere (e.g. Miller *et al*., 1988; Hunt, 1996; Ebel and Nimmo, 2010; Mirus *et al*, 2011; Hemmings *et al*., 2012). Miller *et al*. (1988) studied a perched groundwater system beneath irrigated land on Oahu, Hawaii, using samples from seven boreholes drilled to depths ranging from 12 to 30 m. He found that unsaturated conditions dominated. However, there were also thin, saturated zones of perched water above low-permeability layers interspersed throughout. Some of these layers flowed so slowly that they were not detected in the field, but were found by water content analysis of core samples after the fact. A perched groundwater system on the western flank of Haleakala Volcano has not been previously recognized. Hence, this shallow flow zone likely exists only within the confines of the HC&S plantation as a result of irrigation. The reservoirs and canals on the slope of the HC&S plantation are embedded in and contribute to this down-slope flow. The resistivity pattern for Reservoir 92, on the nearly flat land within the isthmus, shows the thickest low-resistivity layer with no asymmetry with respect to the reservoir. Hence, the flow likely turns vertical in the isthmus and recharges the basal aquifer (Fig. 8).

The sub-soil flow system within the HC&S plantation is likely similar to that observed on Oahu by Miller *et al.* (1988), which consists of sparse, laterally discontinuous, centimeter-scale saturated zones within the saprolite and underlying weathered basalt that is otherwise unsaturated. For this reason, it would be difficult to validate the resistivity results by direct sampling at discrete locations, as is common in resistivity studies of soil hydrology (Hagrey and Michaelsen, 1999; Zhou *et al*., 2001; Garambois *et al*., 2002; Michot *et al*.,

2003; Amidu and Dunbar, 2007). At a minimum, it would require many, continuously cored borings to depths of 20 m or more, which is inconsistent with the reconnaissance nature of this study. Even then, results from similar attempts to estimate hydraulic properties in analogous facture flow systems indicate that estimating bulk properties within an order of magnitude would not be possible (Biggar and Nielsen, 1976; Baker, 2006; Brown *et al*., 2011). Instead, we measured radon levels in the various waters coming in to the plantation and within the irrigation water conveyance system in an effort to find independent evidence of an active sub-soil flow system within the plantation. Using this approach, no evidence for groundwater flow into reservoirs was found. The fact that lower levels of radon were observed in reservoirs than in the supplying canals and chutes indicates that the rate of any groundwater flow into the reservoirs tested must have been low enough that the rate of radon loss caused by decay and degassing in the reservoirs was higher than the rate of any addition by any groundwater infiltration. Significant addition of shallow, down-slope-directed flow of ground water intercepted by the reservoirs would have been indicated by higher reservoir radon levels relative to inflow water from the canal. The opposite was observed. This would be the case if the pressure head on the reservoir bottom was higher than the local head within the flow system. We did note that Reservoirs 22 and 30 had very low water levels at the time they were sampled. The HC&S reservoirs are generally filled just prior to using the water for irrigation. Hence, the water remaining within these reservoirs at the time they were sampled could have been relatively old in comparison to the 3.8 d half life of ^{222}Rn.

In two instances within the canal radon measurements, significant decreases in radon levels occurred in the down-flow direction. This occurred for the samples in the most-upslope Hamakua Ditch (Table 2, Sample 1) and between the end of the first segment and beginning of the second segment tested in Kauhioka Ditch (Table 2, Samples 2 and 3). The lower radon activity at the down-flow sampling locations indicates a loss of radon gas from the water, likely caused by degassing associated with drop structures in the canal present between the two sampling locations. Degassing of radon may occur when the thickness of the water to atmosphere boundary layer is reduced as a function of increased velocity and reduced water depth (Elsinger and Moore, 1983). While not quantified, drop structures were observed in most of the canals sampled and were characterized by fast flowing water with shallow depths; these would be expected to be sites of degassing. Degassing is also likely to occur in the chutes leading from the main canals to the reservoirs, as we found lower radon activity values in the chutes than in the canal water.

The lack of detectable radon in surface water flowing into the plantation from the east side of Haleakala Volcano indicates that radioactive decay rates in the walls and lining of the canals are insufficient to produce detectable radon in the rapidly moving water. Where the down-flow radon activities were significantly higher than up-flow, we conclude that the increase is caused by the infiltration of ground water into the canal from upslope sources. An increase in the radon level by more than a sample standard deviation occurred for one pair of sampling locations (Table 2; Sample 2, Kauhihoka Ditch). This result provides corroborating evidence for down-slope, shallow flow occurring within the plantation. However, when the same ditch was sampled approximately 1.5 km further down-flow, the radon level had dropped back down to a non-detectable level and no significant radon was detected in the segment beyond that point (Table 2, Sample 3, Kauhihoka Ditch). Resistivity Profile 2 crosses Kauhihoka Ditch approximately at the mid-point of this segment. The resistivity pattern on this profile shows evidence for an increase in the thickness of the wet zone immediately upslope of the ditch, and yet this groundwater did not infiltrate into the canal in sufficient quantity to show a statistically significant amount of radon in the canal water. No significant down-flow change in radon levels were observed in the measurements in Lowrie and Haiku Ditches (Table 2, Samples 4 and 5). We conclude from this that, although the shallow flow system may exist throughout the plantation, little of the flow is recaptured by the canal system. It is likely that significant groundwater inflow to the canals can only occur where the thin flow pathways within the saprolite happen to align with cracks in the canal linings, which are also narrow and widely spaced. However, this does not rule out the possibility that water pressure levels within the shallow flow system locally act to retard seepage loss from the canals and reservoirs.

The new conceptual model of down-slope flow of shallow ground water for the HC&S plantation has implications for how measured seepage rates for reservoirs and canals are interpreted and applied to overall estimates of irrigation system losses. Standard practice for estimating irrigation system losses is to characterize parts of the system by lined versus unlined, by crack density within lined components and by the local hydraulic conductivity of surrounding soils. Seepage loss rates are measured for representative components of each category and the results are weighted, typically by wetted area, to estimate overall loss rates (ANCID, 2003; Kaufmann, 2009; Hobza and

Anderson, 2010). The presence of a shallow groundwater system originating upslope of components of the irrigation system further complicates this process. Depending on local head within the groundwater system relative to the head within a particular irrigation system component, permeable components could gain, lose, or hold water. Any positive head within the shallow flow system surrounding the reservoirs and canals will retard seepage loss relative to that which would occur in the absence of a shallow flow system. Hence, an estimate of the local conditions within the shallow groundwater system are needed to interpret seepage measurements on individual irrigation system components, as well as for the use of seepage measurements to estimate the total losses from the overall system.

Conclusions

In this study, we combined electrical resistivity with radon activity measurements within irrigation reservoirs and canals to characterize the shallow groundwater flow system within the HC&S plantation, Maui, Hawaii. Four resistivity profiles where collected along a representative toposequence across the plantation. These profiles show a down-slope-thickening, superficial, low-resistivity layer that we associate with a perched, unsaturated, groundwater flow system. The system appears to move irrigation water down-slope through fracture pathways within the weathered basalt of the Kula Volcanics Formation. Some of this water likely continues down-slope and ultimately recharges the basal aquifer within the isthmus between East and West Maui. The shallow flow system is expected to influence seepage rates from reservoirs and canals, in that loss from the system is expected where the head within reservoirs and canals exceeds local conditions within the flow system, whereas gain is expected where the local head within the flow systems exceeds that within adjacent reservoirs and canals. This means that knowledge of the shallow flow system is needed to estimate water loss rates from the irrigation system.

Acknowledgments

This project was supported by USDA Grant 32110119. We are thankful for logistical help and guidance from Mae Nakahata and Rick Volner, of HC&S.

References

AGI., 2006, Instruction manual for the SuperSting^{TM} with Swift^{TM} automatic resistivity and IP system: Advanced Geosciences, Inc., Austin, Texas, 93 pp.

Amidu, S.A., and Dunbar, J.A., 2007, Geoelectric studies of seasonal wetting and drying of a Texas Vertisol: Vadose Zone Journal, **6**, 511–523.

ANCID., 2003, Open channel seepage & control Vol. 1.4 – Best practice guidelines for channel seepage identification and measurement, 2003: Australian National Committee of Irrigation and Drainage, Tatura, Victoria, Australia, 95 pp.

Apostolopoulos, G., 2012, Marine resistivity tomography for coastal engineering applications in Greece: Geophysics, **77**(3), B97–B105, DOI: 10.1190/GEO2011-0349.1.

Baker, K., 2006, Idaho National Laboratory Vadose Zone Research Park geohydrological monitoring results: Report INL/EXT-05-01044, Idaho National Laboratory, Idaho Falls, Idaho, 19 pp.

Bosch, D.D., Lowrance, R.R., Sheridan, J.M., Williams., and R. G., 2006, Ground water storage effect on streamflow for a southeastern coastal plain watershed: Ground Water, **41**(7), 903–912.

Bouwer, H., 2002, Artificial recharge of groundwater: Hydrology and engineering: Hydrology Journal: **10**, 121–142, DOI: 10.1007/s10040-001-0182-4.

Brown, K.B., McIntosh, J.C., Rademacher, L.K., and Lohse, K.A., 2011, Impacts of agricultural irrigation recharge on groundwater quality in a basalt aquifer system (Washington, USA): A multi-trace approach: Hydrogeology Journal, **19**, 1039–1051.

Burnett, W.C., Peterson, R.N., Santos, I.R., and Hicks, R.W., 2010, Use of automated radon measurements for rapid assessment of groundwater flow into Florida streams: Journal of Hydrology: **380**, 298–304.

Cook, P.G., 2012, Estimating groundwater discharge to rivers from river chemistry surveys: Hydrological Processes, DOI: 10.1002/hyp.9493.

Cook, P.G., Favreau, G., Dighton, J.C., and Tickell, S., 2003, Determining natural groundwater influx to a tropical river using radon, chlorofluorocarbons and ionic environmental tracers: Journal of Hydrology, **277**, 74–88.

Cook, P.G., Lamontagne, S., Berhane, D., and Clark, J.F., 2006, Quantifying groundwater discharge to Cockburn River, southeastern Australia, using dissolved gas tracers ^{222}Rn and SF_6: Water Resources Research, **42**, W10411, DOI: 10.1029/2006WR004921.

Corbett, D.R., Burnett, W.C., Cable, P.H., and Clark, S.B., 1997, Radon tracing of groundwater input into Par Pond, Savannah River Site: Journal of Hydrology, **203**, 209–227.

de Fraiture, C., Molden, D., and Wichelns, D., 2010, Investing in water for food, ecosystems and livilhoods: An overview of the comprehensive assessment of water management in agriculture: Agricultural Water Management, **97**(4), 495–501, DOI: 10.1016/j.agwat.2009.08.015.

Dewandel, B., Gandolfi, J.M., de Condappa, D., and Ahmed, S., 2008, An efficient methodology for estimating irrigation return flow coefficients of irrigated crops at watershed and seasonal scale: Hydrological Processes, **22**, 1700–1712.

Dor, N., Syafalni, S., Abustan, I., Tadza, M., Rahman, A., Nazri, M.A.A., Mostafa, R., and Mejus, L., 2011,

Verification of surface-groundwater connectivity in an irrigation canal using geophysical, water balance and stable isotope approaches: Water Resource Management, **25**, 2837–2853, DOI: 10.1007/s11269-011-9841-y.

Ebel, B.A., and Nimmo, J.R., 2010, Simple estimation of fastest preferential contamination travel times in the unsaturated zone: Application to the Rainer Mesa and Shoshone Mountain, Nevada: Hydrology and Earth Systems Sciences Discussions, **7**, 3879–3930, DOI: 10.51194/hessd-7-3879-2010.

Elsinger, R.J., and Moore, W.S., 1983, Gas exchange in the Pee Dee River based on ^{222}Rn evasion: Geophysical Research Letters, **10**, 443–446.

Engelbert, P.J., Hotchkiss, R.H., and Kelly, W.E., 1997, Integrated remote sensing and geophysical techniques for locating canal seepage in Nebraska: Journal of Applied Geophysics, **38**, 143–154.

Engesgaard, P., Looms, M.C., Kidmose, J., Nilsson, B., and Laier, T., 2010, Spatial distribution of seepage at a flow-through lake: Lake Hampen, Western Denmark: Vadose Zone Journal, **10**, 110–124, DOI: 10.2136/vzj2010.0017.

Engott, J.A., 2006, Assessment of historic ground-water recharge in central and west Maui, Hawaii: M.Sc. thesis, University of Hawaii, Honolulu, Hawaii.

Engott, J.A., and Vana, T.T., 2007, Effects of agricultural land-use changes and rainfall on ground-water recharge in central and west Maui, Hawaii, 1926-2004: U.S. Geological Survey Scientific Investigations Report 2007-5103, 56 pp.

Garambois, S., Sénéchal, P., and Perroud, H., 2002, On the use of combined geophysical methods to assess water content and water conductivity of near-surface formations: Journal of Hydrology, **259**, 32–48.

Gingerich, S.B., 1999a, Ground water and surface water in the Haiku area, east Maui, Hawaii: U.S. Geological Survey Water-Resources Investigations Report 98-4142, 37 pp.

Gingerich, S.B., 1999b, Ground-water occurrence and contribution to stream flow, northeast Maui, Hawaii: Water-Resources Investigations Report 99-4090, U.S. Department of the Interior, U.S. Geological Survey, Honolulu, Hawaii, 70 pp.

Gingerich, S.B., 2008, Ground-water availability in the Wailuku Area, Maui, Hawaii: USGS Scientific Investigations Report 2008-5236, U.S. Department of the Interior, U.S. Geological Survey, Reston, Virginia, 95 pp.

Hagrey, S.A.A., and Michaelsen, J., 1999, Resistivity and percolation study of preferential flow in vadose zone at Bokhorst, Germany: Geophysics, **64**, 746–753.

Ham, J.M., and Baum, K.A., 2009, Measuring seepage from waist lagoons and earthen basins with an overnight water balance test: Transactions of the American Society of Agricultural and Biological Engineers, **52**(3), 835–844.

Hemmings, B., Whitaker, F., and Gottsmann, J., 2012, Initial investigations of the productive perched aquifers on the volcanic island of Montserrat: *in* Proceedings, TOUGH Symposium 2012, Lawrence Berkeley National Laboratory, Berkeley, CA, September 17–19, 2012, 8 pp.

Hobza, C.M., and Anderson, M.J., 2010, Quantifying canal leakage rates using a mass-balance approach and heat-based hydraulic conductivity estimates in selected irrigation canals, Western Nebraska, 2007 through 2009: U.S. Department of the Interior, U.S. Geological Survey, Scientific Investigations Report 2010-5226, Reston Virginia, 44 pp.

Hotchkiss, R.H., Wingert, C.B., and Kelly, W.E., 2001, Determining irrigation canal seepage with electrical resistivity: Journal of Irrigation and Drainage Engineering, **127**(1), 20–26, DOI: 10.1061/(ASCE)0733-9437(2001)127:1(20).

Humphreys, G., Foo, D.Y., Tickell, S., Jolly, P., and Chin, D., 2002, Planning to manage sustainably: Natural resource geophysics as part of resource assessment: Exploration Geophysics, **33**(2), 103–109.

Hunt, C.D. Jr., 1996, Geohydrology of the island of Oahu, Hawaii, regional aquifer-system analysis: U.S. Geological Survey Professional Paper 1412-B, Denver, CO., 54 pp.

Izuka, S.K., 1992, Geology and stream infiltration of North Halawa Valley, Oahu, Hawaii: U.S. Geological Survey, Water-Resources Investigations Report 91-4197, Honolulu, Hawaii, 21 pp.

Izuka, S.K., Oki, D.S., and Chen, C., 2005, Effects of irrigation and rainfall reduction on grad-water recharge in the Lihue Basin, Kaui, Hawaii: U.S. Geological Survey Scientific Investigations Report 2005-5146, Honolulu, Hawaii, 48 pp.

Kaufmann, R., 2009, Reclamation, managing water in the West, geophysical survey for canal seepage Yuma Area Demonstration Project: U.S. Department of the Interior, Bureau of Reclamation, Yuma, Arizona, 20 pp.

Khan, S., Dharma, D., and Mushtaq, S., 2010, Predicting water allocations and trading process to assist water markets: Irrigation and Drainage, **59**(4), 388–403, DOI: 10.1002/ird.535.

Khan, S., Tariq, R., Yuanlai, C., and Blackwell, J., 2006, Can irrigation be sustainable?: Agricultural Water Management, **80**, 87–99, DOI: 10.1016/j.agwat.2005.07.006.

Mattice, M.D., 1981, Geothermal and ground water exploration on Maui, Hawaii, by applying D.C. electrical soundings: M.Sc. thesis, University of Hawaii, Manoa, Hawaii.

McDonald, H.R., and Wantland, D., 1960, Geophysical procedures in ground water study: ASCE Journal of Irrigation and Drainage, **86**(3), 13–26.

Miller., M. W., Green, R.W., Peterson, F.L., Jones, R.C., and Loague, K., 1988, Hydrogeologic characteristics of subsoil and saprolite and their relation to contaminant transport, central Oahu, Hawaii: Technical Report No. 178, Water Resource Research Center, University of Hawaii, Manoa, Hawaii, 76 pp.

Minsley, B.J., Smith, B.D., Hammack, R., Sams, J.I., and Veloski, G., 2010, Geophysical characterization and monitoring of subsurface drip irrigation, Power River Basin, Wyoming, USA: *in* Expanded Abstracts, 21st Geophysical Conference and Exhibition, Australian Society of Exploration Geophysicists (ASEG), August

22-26, 2010, Sydney, Australia, **1**, 1–4, DOI: 10.1071/ASEG2010ab104.

Mirus, B.B., Perkins, K.S., and Nimmo, J.R., 2011, Assessing controls on perched saturated zones beneath the Idaho Nuclear Technology and Engineering Center, Idaho: Scientific Investigations Report 2011-5222, U.S. Department of the Interior, U.S. Geological Survey, Reston, Virginia, 20 pp.

Mullinger, N.J., Binley, A.M., Pates, J.M., and Crook, N.P., 2007, Radon in chalk streams: Spatial and temporal variation of groundwater sources in the Pang and Lambourn catchments, UK: Journal of Hydrology, **339**, 172–182.

Mushtaq, S., Chen, C., Mohsin, H., Maroulis, J., and Gabriel, H., 2012, The economic value of improved agrometeorological information to irrigators amid climate variability: International Journal of Climatology, **32**(4), 567–581, DOI: 10.1002/joc.2015.

Priest, S., 2004, Evaluation of ground-water contribution to streamflow in coastal Georgia and adjacent parts of Florida and South Carolina: U.S. Department of the Interior, U.S. Geological Survey, Scientific Investigations Report 2004-5265, U.S. Geological Survey, Reston, Virginia, 40 pp.

Rosenberry, D.O., Toran, L., and Nyquist, J.E., 2010, Effect of surficial disturbance on exchange between groundwater and surface water in nearshore margins: Water Resources Research, **46**, W06518, DOI: 10.1029/2009WR008755.

Safeeq, M., and Fares, A., 2012, Hydrologic response of a Hawaiian watershed to future climate change scenarios: Hydrological Processes, **26**, 2745–2764, DOI: 10.1002/hyp.8328.

Stearns, H.T., and MacDonald, G.A., 1942, Geology and ground-water resources of the island of Maui, Hawaii: Bulletin 7, U.S. Department of the Interior, U.S. Geological Survey, Honolulu, Hawaii, 344 pp.

Swarzenski, P.W., and Izbicki, J.A., 2009, Coastal groundwater dynamics off Santa Barbara, California: Combining geochemical traces, electromagnetic seep meters and electrical resistivity: Estuarine: Coastal and Shelf Science, **83**, 77–89.

Toran, L., Johnson, M., Nyquist, J., and Rosenberry, D., 2010, Delineating a road-salt plume in lakebed sediments using electrical resistivity, piezometers and seepage meters at Mirror Lake, New Hampshire, U.S.A.: Geophysics, **75**(4), WA75–WA83, DOI: 10.1190/1.3467505.

USDIBR., 1963Linings for irrigation canals, U.S. Department of the Interior, Bureau of Reclamation, U.S. Government Printing Office, Washington, D.C., 149 pp.

Wada, K., Henmi, T., Yoshinaga, N., and Patterson, S.H., 1972, Imogolite and Allophane formed in saprolite of basalt on Maui, Hawaii: Clays and Clay Minerals, **20**, 375–380.

Wada, Y., Wisser, D., Eisner, S., Flörke, M., Gerten, D., Haddeland, I., Hanasaki, N., Masaki, Y., Portmann, F.T., Stacke, T., Tessler, Z., and Schewe, J., 2013, Multimodel projections and uncertainties of irrigation water demand under climate change: Geophysical Research Letters, **40**(17), 4626–4632, DOI: 10.1002/grl.50686.

Wantland, D., 1953, Experimental resistivity investigations on canal seepage problems: Geology Report No. 125, U.S. Department of the Interior, Bureau of Reclamation, Denver, Co., 118 pp.

Watt, J., 2008, The effect of irrigation on surface-ground water interactions: Quantifying time dependent spatial dynamics in irrigation systems: Ph.D. dissertation, Charles Sturt University, Wodonga, New South Wales, Australia, 265 pp.

Zhou, Q.Y., Shimada, J., and Sato, A., 2001, Three-dimensional spatial and temporal monitoring of soil water content using electrical resistivity tomography: Water Resources Research, **37**, 273–285.